Ecotoxicology and Environmental Safety 311 (2026) 119873

Contents lists available at ScienceDirect

Ecotoxicology and Environmental Safety

journal homepage: www.elsevier.com/locate/ecoenv

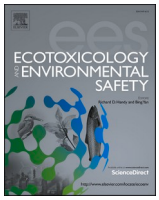

# Critical evaluation of enzymatic extraction for quantification of europium-doped polystyrene nanoplastics in tomato tissues by single particle ICP-MS

Harshit Sahai [a,b,*], Pia Leban [c,d], Ester Heath [c,d], Nina Kacjan Maršić [e], Špela Železnikar [e], Matejka Podlogar [f], Tina Radošević [f], María Jesús Martinez Bueno [b], Janja Vidmar [c,d,**]

[a] Experimental Station of Arid Zones, The Spanish National Research Council (CSIC-EEZA), Ctra. de Sacramento s/n, La Cañada de San Urbano, Almería 04120, Spain
[b] Research Group "Pesticide Residues", Department of Chemistry and Physics, Research Centre for Mediterranean Intensive Agrosystems and Agri-Food Biotechnology (CIAMBITAL), University of Almería, Agri-Food Campus of International Excellence (ceiA3), Almería 04120, Spain
[c] Jožef Stefan Institute, Department of Environmental Sciences, Jamova cesta 39, Ljubljana 1000, Slovenia
[d] Jožef Stefan International Postgraduate School, Jamova cesta 39, Ljubljana 1000, Slovenia
[e] Biotechnical Faculty, Department of Agronomy, University of Ljubljana, Jamnikarjeva 101, Ljubljana 1000, Slovenia
[f] Jožef Stefan Institute, Department for Nanostructured materials, Jamova cesta 39, Ljubljana 1000, Slovenia

ARTICLE INFO

Edited by: Richard Handy

*Keywords:*
Nanoplastics
Polystyrene
Enzymatic extraction
Single particle ICP-MS
Tomato
Bioaccumulation

ABSTRACT

This study critically evaluates an analytical approach combining enzymatic extraction and single particle ICP-MS (spICP-MS) for quantifying europium-doped polystyrene nanoplastics (Eu-PS-NPs) bioaccumulated in tomato tissues. Optimization of extraction parameters identified citrate buffer at pH 6.5 and a digestion temperature of 37 °C as the most effective extraction conditions, while maintaining particle stability. Experiments with spiked tomato tissues demonstrated that extraction efficiency is highly tissue-specific, with optimal digestion of 24 h for stem, leaf, and fruit, and 36 h for root tissues, and enzyme concentrations ranging from 10 to 100 mg per sample. Under optimized conditions, good extraction recoveries (85 – 116 %) were achieved for particle number and mass concentrations, particle size and mass, and total Eu mass, with the majority of extracted Eu associated with NPs and around 10 % as ionic Eu. In contrast, analysis of tomato samples exposed to Eu-PS-NPs during their growth revealed substantially lower and tissue-dependent extraction recoveries. Root and stem tissues yielded only 18 – 32 % of total Eu mass concentration, while leaves showed recoveries $\leq$ 21 % under most extraction conditions. Fruit samples exhibited higher apparent recoveries (66 – 80 % after 24 h digestion), likely due to the acidic environment promoting Eu leaching from NPs. Across all exposed tissues, ionic Eu fraction dominates (reaching up to 97 % in fruits), indicating extensive leaching from Eu-PS-NPs in the tomato plants. These findings underscore the importance of accounting for matrix effects, metal leaching, and the limitation of extrapolating recoveries from spiked controls to exposed samples when interpreting spICP-MS data from plant exposure studies with metal-doped NPs.

## 1. Introduction

Global plastic waste is expected to nearly triple, from 353 million tons (Mt) in 2019 to about 1014 Mt by 2060 (OECD, 2024), with agriculture contributing 12.5 Mt, predominantly through the use of films for mulch, silage, and greenhouses, as well as in irrigation systems, twines, nets, and pipes (FAO, 2021). Although agricultural plastics can enhance crop productivity and reduce water and agrochemical demands, their use contributes to long-term soil contamination from the release of micro- and nanoplastics (MNPs), which have been extensively reported in agricultural soils worldwide (Büks and Kaupenjohann, 2020), with a global stock estimated at 1.5–6.6 Mt (Maddela et al., 2023; Kedzierski et al., 2023). The abundance of MNPs in soil is influenced by multiple factors, including agricultural practices, soil management, land use,

* Corresponding author at: Research Group "Pesticide Residues", Department of Chemistry and Physics, Research Centre for Mediterranean Intensive Agrosystems and Agri-Food Biotechnology (CIAMBITAL), University of Almería, Agri-Food Campus of International Excellence (ceiA3), Almería 04120, Spain.
** Corresponding author at: Jožef Stefan Institute, Department of Environmental Sciences, Jamova cesta 39, Ljubljana 1000, Slovenia.
*E-mail addresses:* harshitsahai@ual.es (H. Sahai), janja.vidmar@ijs.si (J. Vidmar).

https://doi.org/10.1016/j.ecoenv.2026.119873
Received 1 October 2025; Received in revised form 4 February 2026; Accepted 9 February 2026
Available online 11 February 2026

proximity to industrial or urban areas, roads and highways, application of biosolids or sludge, the use of treated irrigation water, and the history of plastic use in agriculture (Sahai et al., 2025). Among these, irrigation water has been identified as one of the prominent sources of MNP contamination in agricultural soils (Guo et al., 2023; Pérez-Reverón et al., 2022; Ragoobur et al., 2021). In response to such concerns, the European Union's recent Directive (EU) 2024/3019 concerning urban wastewater treatment (Directive, 2025) mandates member states to monitor and reduce MP pollution in urban wastewater and sludge, particularly when reused in agriculture, to align with the EU's broader zero-pollution objectives.

Beyond their environmental persistence, MNPs can have various negative effects on soil ecosystems, soil biota and plant health (Tian et al., 2022). Of growing concern is the uptake, translocation, and bioaccumulation of MNPs by crops. Recent studies have demonstrated the uptake of MNPs in a variety of plants, including *Triticum aestivum* (wheat) (Taylor et al., 2020; Gong et al., 2021), *Lactuca sativa* (lettuce) (Gong et al., 2021; Lian et al., 2021), *Arabidopsis thaliana* (thale cress) (Taylor et al., 2020; Sun et al., 2020), *Pisum sativum* (pea) (Kim et al., 2022), *Oryza sativa* (rice) (Liu et al., 2022), *Daucus carota* (carrot) (Dong et al., 2021), *Murraya exotica* (orange jasmine) (Zhang et al., 2019), *Raphanus sativus* (radish) (Gong et al., 2021; Tympa et al., 2021), *Zea mays* (maize) (Gong et al., 2021; Sun et al., 2021), *Allium cepa* (onion) seeds (Giorgetti et al., 2020a), *Cucumis sativus* (cucumber) (Li et al., 2021a, 2021b) and *Vicia faba* (fava bean or broad bean) (Jiang et al., 2019). The accumulation of MNPs in plants may impair plant health, including its nutritional quality, biomass production, and decrease crop production, as well as open another pathway for MNPs to enter the human food chain, affecting food safety and human health. Of particular concern are nanoplastics (NPs), which are more readily absorbed by plants and pose greater ecological risks than MPs. This issue has led to a surge in research efforts focused on the uptake of NPs by plants and their subsequent impact.

Detecting and quantifying NPs in plant tissues remains a significant analytical challenge due to their small size, irregular shape, and varied polymeric compositions (Yu et al., 2024). Analytical techniques such as confocal laser scanning microscopy (CLSM) (Taylor et al., 2020; Sun et al., 2020; Kim et al., 2022; Liu et al., 2022; Li et al., 2021a, 2020), transmission electron microscopy (TEM) (Giorgetti et al., 2020b), time-resolved optical imaging/fluorescence imaging and scanning electron microscopy (SEM) (Luo et al., 2022a), pyrolysis gas chromatography/mass spectrometry (Py-GC/MS) (Li et al., 2021b), inductively coupled plasma mass spectrometry (ICP-MS) alone (Wang et al., 2022) or coupled with laser ablation (LA) (Wang et al., 2024) have been employed so far, though each suffers from particular limitations. For example, fluorescence-based techniques may be limited by high (size) detection thresholds and background interference, while most microscopic imaging techniques lack quantification and can analyze only small, potentially unrepresentative tissue areas. In contrast, (LA)ICP-MS provides a quantitative, sensitive, and interference-free (spatial) analysis of NPs that are either intentionally labelled with metal or contain metal-based plastic additives, though it does not allow particle-by-particle counting. In this context, single particle ICP-MS (spICP-MS) has emerged as a promising technique for the detection and quantification of bioaccumulated engineered nanoparticles (ENPs) in plant tissues. It offers particle-specific data on number concentration, mass concentration, and size distribution, with high sensitivity and low detection limits. SpICP-MS has been successfully used to detect a range of metal-containing ENPs, such as $CeO_2$, Pd, Au, CuO, and Pt-NPs in various plants (Dan et al., 2015; Kińska et al., 2018; Keller et al., 2018; Jiménez-Lamana et al., 2016). Besides ENPs, spICP-MS has recently been explored for detecting MPs by relying on the detection of carbon; however, due to high carbon background levels and limited carbon sensitivity, its application is typically limited to particles larger than ~1 μm (Laborda et al., 2013; Bolea-Fernandez et al., 2020). To enable the analysis of smaller plastic particles by spICP-MS, metal-labelled NPs can be used, where trace metals (e.g., Eu, Ag, Au) serve as detectable proxies, allowing for sensitive analysis of NPs well below the carbon detection threshold (Lee et al., 2014; Caceres).

Employing metal-doped NPs in controlled laboratory-scale exposure studies offers a promising approach to better understand the mechanisms underlying NPs uptake and bioaccumulation in plants. To date, the uptake and bioaccumulation of metal-doped NPs in plants has been assessed solely through bulk metal analysis following acid digestion and conventional ICP-MS (Li et al., 2021b; Luo et al., 2022b). This approach lacks particle-specific information, limiting insights into critical parameters such as particle size and number, factors that govern their behaviour, bioavailability, and potential toxicity in plants. While spICP-MS offers the capability to overcome these limitations, its application in plant systems remains unexplored. A major barrier towards standardized methods is the absence of extraction protocols capable of isolating metal-doped NPs from plant tissues without compromising their physicochemical integrity. Existing digestion methods, primarily optimized for the extraction and spICP-MS analysis of ENPs in plants, have utilized enzymatic treatment, often using Macerozyme R-10 (Wang et al., 2022; Dan et al., 2015; Keller et al., 2018; Jiménez-Lamana et al., 2016; Wei et al., 2021) or acid digestion (Luo et al., 2022a; Kińska et al., 2018). However, when applied to NPs, acidic conditions can degrade specific polymers, such as polyamide and polyurethane, altering their chemical structure or leading to their agglomeration (Enders et al., 2017). An alternative approach involving alkaline digestion using tetramethylammonium hydroxide (TMAH), followed by cellulose precipitation with ethanol and ultrasonic leaching with dichloromethane, has been reported for the extraction of metal-labelled NPs from cucumber (Li et al., 2021b) and lettuce (Li et al., 2023). The effectiveness of this extraction method was evaluated by Py-GC/MS analysis and further validated by conventional ICP-MS measurements. Another alkaline digestion protocol based on TMAH has also been reported to achieve quantitative recovery of metal-doped PS NPs from zebrafish tissues, enabling subsequent analysis by single-particle ICP-MS (Lai et al., 2025). However, there is a need to develop an extraction protocol specifically tailored for spICP-MS analysis of metal-doped NPs in plants, to enable accurate particle-specific quantification, thus deepening the mechanistic understanding of nanoparticle–plant interactions.

The objective of this research was to assess the feasibility of enzymatic extraction for isolating europium (Eu)-doped PS nanoparticles from tomato samples, followed by their quantification and size characterization utilizing spICP-MS. In this study, we systematically examine the influence of various parameters, such as buffer pH, digestion temperature, digestion time, and enzyme concentration, on the extraction efficacy from tomato samples spiked with known concentrations of Eu-doped PS NPs. Based on recovery rates obtained for particle concentration and size in spiked samples, the optimal extraction parameters are identified. Additionally, we evaluate the effectiveness of the extraction protocol on tomato samples that were exposed to Eu-doped PS NPs throughout their growth and report the most favourable sample pretreatment conditions based on calculated total Eu extraction recoveries. Lastly, we emphasize the differences in the applicability of this method for extracting Eu-doped PS NPs from spiked tomato samples and tomato samples exposed to NPs under real exposure scenarios, while also addressing its limitations.

## 2. Materials and methods

### 2.1. Reagents and materials

Ultrapure water (18.2 MΩcm) was obtained using the Milli-Q® ultrapure water system (Millipore, Bedford, MA, USA). Ionic Europium (Eu) ICP standard, containing 1000 mg/L of Eu as $Eu_2O_3$ in 2–3 % $HNO_3$, and ionic Gold (Au) ICP standard, containing 1000 mg/L of Au as H($AuCl_4$) in 7 % HCl, were supplied as Certipur®, Supelco, from Merck KGaA (Darmstadt, Germany). Carboxyl Europium Chelate polystyrene

NPs, hereafter referred to as Eu-PS-NPs, were purchased from Bangs Laboratories Inc. (USA). The stock suspension was supplied as 1 % solids (w/v) in deionized water with 0.05 % sodium azide, and contained $2.322 \times 10^{12}$ particles/mL with a mean diameter of 198 nm. According to the manufacturer's data sheet, the material consists of carboxyl-functionalized PS NPs containing an internal Eu (III) chelate label and a PS-COOH surface suitable for covalent coupling. Lanthanide-doped PS particles prepared this way are generally not metal-core particles; rather, Eu is present as an organic chelate complex dispersed within the PS matrix, typically enriched toward the outer region where carboxyl groups are located, effectively resulting in a PS core with an Eu-rich outer layer (Liang et al., 2015). The Eu mass fraction within a PS particle was determined to be 1.67 % by using Equations S1 and S2. Gold nanoparticle (AuNPs) standard (NanoXact™) was purchased from nanoComposix, Inc. (CA, USA) as an aqueous suspension in 2 mM sodium citrate. The AuNPs had a mean diameter of 51 ± 5 nm, a mass concentration of 0.053 mg/mL, a hydrodynamic diameter of 54 nm, and a zeta potential of −46 mV. Citrate buffer solutions were prepared using citric acid ($C_6H_8O_7$) and sodium citrate dihydrate ($Na_3C_6H_5O_7{\cdot}2H_2O$, ACS reagent, >99.0 %), purchased from Sigma-Aldrich (MO, USA). Pectinase from *Rhizopus* sp. (Macerozyme R-10), with an optimal activity of 400–800 units/g solid reported at pH 4.0, was also obtained from Sigma-Aldrich. True Rinse ICP-MS Washout Solution, containing 2 % v/v HCl and 0.5 % w/v Thiourea, was purchased from Inorganic Ventures (VA, USA). Nitric acid (67–69 % wt. $HNO_3$) was purchased from Carlo Erba Reagents (Italy), while hydrochloric acid (30 % wt. HCl), hydrofluoric acid (40 % wt. HF), and hydrogen peroxide (30 % wt·$H_2O_2$) were obtained from Merck. The standard reference material SRM 1570a (Spinach Leaves, NIST, USA; Eu reference mass fraction 0.0055 ± 0.0010 mg/kg) was used to verify the accuracy of total Eu concentration measurements in digested tomato tissues. The Hoagland Arnon nutrient solution (Table S1) was prepared as described by Resh using potable water (Resh, 2025).

### 2.2. Plant cultivation

Tomato plants (*Solanum lycopersicum L. cv. Rally*) were grown hydroponically for five weeks in plastic tanks in a greenhouse located at the Biotechnical Faculty, University of Ljubljana, under monitored environmental conditions using a USB temperature and humidity data logger (DL-121TH Volcraft, Hirschau, Germany). The mean daily air temperature was between 13 °C and 28 °C, and the relative humidity was between 45 % and 85 %. The seedlings were cultivated in peat substrate, and when the plants had five fully developed leaves (BBCH105), they were transferred to the Aerofarm hydroponic system (Terra Aquatica, Italy), which consisted of a tank filled with 40 L of Hoagland – Arnon nutrient solution. The air pump was used to aerate the nutrient solution. Each tank containing three tomato seedlings was covered with inert polyester foam. One tank served as a control with tomatoes exposed to the nutrient solution only, while the others contained plants exposed to the nutrient solution spiked with 1 mg/L of Eu-PS-NPs. The pH of the nutrient solution was adjusted weekly to 7.0 using nitric acid. Due to plant transpiration, the nutrient solution was replenished weekly to 40 L. The spiked nutrient solution used for replenishment contained the same concentration of Eu-PS-NPs as those present at the start of the experiment. When plants reached the stage of the first mature fruit (BBCH 809), samples were carefully collected, divided into roots, stems, leaves, and fruits, and dried in an oven at 60°C for 48 h. The dried samples were ground in a mortar with the addition of liquid nitrogen to powder and stored in sealed vials for further analysis.

### 2.3. Optimization of enzymatic extraction using spiked tomato samples

Enzymatic extraction of Eu-PS-NPs from tomato samples was optimized through a sequence of distinct phases, including an initial stage `homogenization´, wherein 25 mg of plant sample (dried and milled) was mixed with 8 mL of 2 mM citrate buffer in a 15 mL Falcon tube. The resultant mixture was subjected to agitation on a rotary shaker (Edmund Bühler 181 GmbH, Germany) at 100 rpm for 5 min to promote effective mixing. In the subsequent digestion stage, 2 mL of Macerozyme R-10 enzyme solution was added to the sample and allowed to incubate within a temperature-regulated rotary shaker. Once complete, the samples underwent centrifugation or settling to remove any residual plant debris. The supernatant was collected and diluted with Milli-Q water to achieve an optimal particle concentration ($2 \times 10^6 - 10^8$ particles/L) for the spICP-MS analysis.

The optimization of the citrate buffer pH during the homogenization stage, temperature during the digestion stage, and post-digestion step is provided in Supplementary Data Text S1. In brief, the impact of three citrate buffer pH values (4.5, 5.5, and 6.5) and two digestion temperatures (25°C and 37°C) on particle stability was assessed by incubating 25 ng/L of Eu-PS-NPs (expressed as Eu mass concentration) in citrate buffer solutions for 24 h. Particle number and mass concentrations, as well as particle diameter and mass obtained by spICP-MS were compared to those of the original Eu-PS-NPs water suspensions.

For the optimization of digestion time and enzyme concentration, spiked tomato samples were subjected to two different digestion times (24 h and 36 h) and three different enzyme concentrations prepared in a 2 mL aqueous solution (10 mg/sample, 50 mg/sample, and 100 mg/sample). For this purpose, control tomato tissues were spiked with Eu-PS-NPs at 10 mg/kg (root) and 10 μg/kg (stem, leaf, fruit) (See Supplementary Data Text S2). Finally, seven different combinations of post-digestion stage (30 min settling, and centrifugation at 1000 rpm for 3 min, 1000 rpm for 5 min, 2000 rpm for 3 min, 2000 rpm for 5 min, 4000 rpm for 3 min and 4000 rpm for 5 min) were evaluated using control root samples spiked with Eu-PS-NPs at 10 mg/kg (Supplementary Data Text S1). Extraction recoveries were calculated by comparing the relevant parameters of the extracted Eu-PS-NPs obtained by spICP-MS (particle number/mass concentrations, median particle diameter/mass) to those of the spiked Eu-PS-NPs solution. Total Eu mass extraction recovery for spiked samples was determined by comparing the total extractable Eu mass concentration (including Eu in both nanoparticulate and ionic forms) determined by spICP-MS with the Eu mass concentration spiked into the control tomato samples.

### 2.4. Optimization of enzymatic extraction using exposed tomato samples

The effectiveness of the enzymatic extraction was also evaluated for tomatoes exposed to Eu-PS-NPs as described in Section 2.2 (hereafter referred to as "exposed tomato samples"). All enzymatic extraction and spICP-MS parameters were kept consistent with the experiments involving spiked samples. Briefly, 25 mg of the exposed tomato sample (dried and milled) was mixed with 8 mL of citrate buffer (pH 6.5) in a 15 mL Falcon tube, agitated on a rotary shaker at 100 rpm for 5 min, followed by the addition of 2 mL solution containing 10 mg, 50 mg, or 100 mg Macerozyme R-10 enzyme (in separate batches). This mixture was allowed to incubate at 37°C for 24 or 36 h (in separate batches). Digested samples were allowed to settle for 30 min, after which the supernatant was collected and diluted to obtain the optimal particle concentration for spICP-MS analysis. All experiments were conducted in triplicate. Total Eu mass extraction recoveries for exposed tomato samples were determined by comparing the total extractable Eu mass concentration (including Eu in both nanoparticulate and ionic forms) determined by spICP-MS with the Eu mass concentration obtained using ICP-MS after microwave-assisted digestion of the sample.

### 2.5. spICP-MS analysis of the extracted Eu-PS-NPs

The Eu-PS-NPs in extracted tomato samples were measured using spICP-MS on an Agilent 7900 ICP-MS system (Santa Clara, CA, USA) equipped with a MicroMist nebulizer. The analysis was conducted in time-resolved mode with a sampling period of 0.0001 s and a total

acquisition time of 60 s per sample, targeting the Eu isotope at *m/z* of 153 to detect europium-labelled PS NPs. Detailed instrumental parameters are provided in Table S2.

Quantification was performed based on a calibration curve obtained using ionic Eu standard solutions prepared in 0.1 % $HNO_3$ aqueous solution with Eu mass concentrations ranging from 0.5 to 10 ng/mL. The calibration curve was used to calculate the particle mass, which was converted to mass-equivalent PS particle diameter based on the known Eu mass fraction in Eu-PS-NPs (1.67 %) and polystyrene density of spherical particles (1.06 g/cm$^3$). Transport efficiency was calculated using the particle size method by analyzing the AuNPs suspension with a known average particle diameter prepared in water (132 ng/L) and ionic Au standards prepared in True Rinse solution (0.5 – 5 ng/mL). An accurate sample flow rate was determined for each analysis using the gravimetric method, and the rinsing procedure with 1-min aspiration of 4 % $HNO_3$ acid and water after each analysis. The acquired data were processed using the Single Nanoparticle Application Module in the MassHunter 5.2 Workstation Software (Agilent Technologies). The same threshold, manually selected to achieve a symmetrical particle size distribution while excluding background signals, was applied to all samples to ensure comparability among treatments. The Eu mass fractions associated with the nanoparticulate and ionic forms were determined by quantifying their respective contributions to the total Eu mass concentration. The total Eu mass concentration was calculated by averaging the signal intensity across the entire measurement window, capturing both discrete particle events and the continuous background signal corresponding to dissolved Eu.

### 2.6. Determination of total Eu mass concentration in tomato samples

The total Eu mass concentration in digested tomato tissues was determined using ICP-MS analysis following a microwave-assisted digestion. Briefly, 0.2 g of plant sample was weighed into a Teflon vessel, and 7 mL of 30 % (w/w) $H_2O_2$, 1 mL of 68 % (w/w) $HNO_3$, and 0.05 mL of 40 % (w/w) HF were added. The vessels were left open for 30 min to allow initial reactions. The samples were then digested using the CEM Corporation MARS 5 Microwave System (Matthews, NC, USA) as follows: 20 min ramp to 140 °C, a 2 min hold at 140 °C, followed by a 15 min ramp to 200 °C and a 60 min hold at 200 °C, with a subsequent cooling period of 30 min. After digestion, the solutions were transferred to 30 mL tubes and diluted to 20 mL with Milli-Q water. The digestion procedure was validated using SRM 1570a processed under identical conditions. ICP-MS analysis was carried out in He mode, targeting Eu isotope at *m/z* of 153. External calibration was performed using ionic Eu standards prepared in 3.4 % $HNO_3$ in a concentration range of 0.005 – 20 ng/mL, and an online internal standardization using a 25 ng/mL solution of Rh, Ir, and Bi. Blanks and SRM 1570a were included in each batch for quality control.

### 2.7. SEM and DLS analysis

The shape and size of the Eu-PS-NPs were investigated by scanning electron microscope (SEM, Verios 4 G HP, Thermo Fisher Scientific Inc., USA). Eu-PS-NP particles were dispersed in distilled water, dropped onto an aluminum SEM holder, and dried at 25°C and 60°C to assess any changes in particle morphology resulting from exposure to 60°C during the drying of tomato samples. The behaviour of Eu-PS-NPs (10 mg/L PS, corresponding to 0.167 mg/L Eu) was assessed in Milli-Q water (pH 7.7) and citrate buffer at varying pH (4.5, 5.5, and 6.5). Zeta potential, hydrodynamic diameter, median diameter (D50 intensity), and polydispersity index (PDI) were measured as indicators of particle stability and size distribution using dynamic light scattering (DLS Litesizer 500, Anton Paar GmbH, Graz, Austria).

### 2.8. Statistical analyses

Significant differences were assessed using a paired two-sample *t*-test, with $p \leq 0.05$ considered statistically significant.

## 3. Results and discussion

### 3.1. Characterisation of Eu-PS-NPs

The basic characteristics of the Eu-PS-NPs in water suspension are presented in Table 1.

The results of the spICP-MS analysis were in good agreement with the expected parameters (as provided by standard's manufacturer), including particle number (92.6 %) and mass concentrations (88.1 %), median particle diameter (97.1 %), and median particle mass (91.4 %). These results demonstrate that the spICP-MS method, utilizing time-resolved analysis of the Eu isotope signal, provides a robust, accurate, and reliable approach for their quantification and size characterization. Also, the Eu mass concentration associated with particles accounted for 88.1 % of the total Eu mass concentration, while the ionic Eu mass fraction was 10.5 ± 0.3 %, indicating the amount of Eu already leached from NPs in water suspension. Zeta potential analysis confirmed the stability of Eu-PS-NPs in water, revealing a strongly negative surface charge that promotes electrostatic repulsion. The hydrodynamic diameter (256 ± 11 nm) and median diameter (221 ± 2 nm) obtained by DLS, which measures the size of the core particles along with any surface coating and solvation layers, were, as expected, larger than the median particle diameter obtained by spICP-MS (192.1 nm), with a PDI of 22 %, indicating a moderately uniform size distribution.

In citrate buffers (see Table S3), Eu-PS-NPs exhibited negative zeta potential values ranging from - 54.5 ± 1.1 mV at pH 6.41 to - 37.8 ± 1.1 mV at pH 4.53. An observed trend of decreasing negative charge with decreasing pH is consistent with the protonation of surface carboxyl (COO-) functional groups or their interaction with sodium cations present in the citrate buffer. The less negative zeta potential at pH 4.53 suggests reduced electrostatic repulsion among particles, which may promote particle aggregation and sedimentation. Accordingly, the hydrodynamic diameter increased progressively with decreasing pH of the citrate buffer (from 277 ± 1 nm at pH 6.41–284 ± 6 nm and 313 ± 2 nm at pH 5.42 and pH 4.53, respectively), suggesting a greater tendency for aggregation at lower pH values. The median diameter (D50) values followed a similar trend, with PDI values remaining relatively consistent across all media (ranging from 20 % to 22 %), indicating a sufficiently uniform size distribution across all pH levels despite changes in size and aggregation behaviour.

### 3.2. Optimization of enzymatic extraction parameters using spiked tomato samples

#### 3.2.1. Optimization of citrate buffer pH and digestion temperature

The effect of citrate buffer pH (4,5, 5.5, and 6.5) and digestion temperature (25 and 37°C) on the Eu-PS-NPs stability was evaluated as

**Table 1**
Summary of the Eu-PS-NPs characteristics in water suspension. Results are presented as mean ± STD (N = 3). Values in [] represent recoveries, calculated by comparing spICP-MS values with expected values.

| Eu-PS-NPs parameter | Determined value |
|---|---|
| Particle number concentration (particles/L) | (5.4 ± 3.2) x 10$^7$ [92.6 ± 5.5 %] |
| Eu particle mass concentration (ng/L) | 220.2 ± 11.6 [88.1 ± 4.6 %] |
| Median particle diameter (nm) | 192.1 ± 1.2 [97.1 ± 0.7 %] |
| Median PS particle mass (ag) | 3938 ± 69 [91.4 ± 2.0 %] |
| Hydrodynamic diameter (nm) | 256 ± 11 |
| Median diameter (D50 intensity, nm) | 221 ± 2 |
| PDI (%) | 22 ± 2 |
| Zeta potential (mV) | -47.1 ± 0.6 |

described in Section 2.3. Recovery values for all treatments are shown in Fig. 1a, with detailed data in Table S4. Incubation for 24 h in citrate buffer at pH 6.5, at either 25 or 37°C, gave the highest recovery (> 91 % for particle number and mass concentrations, and 100 % for median particle diameter and mass). Other treatment conditions generally gave 10 – 25 % lower recoveries at pH 4.5 and 5.5, regardless of temperature, suggesting that more acidic conditions hinder extraction recovery, due to particle aggregation or degradation. However, pH-induced aggregation did not compromise particle size recovery, which remained near 100 % under acidic conditions. Namely, aggregation produced larger agglomerates that are more prone to sedimentation or inefficient nebulization, leading to under detection by spICP-MS. Consequently, particle number concentrations decreased while the measured particle size of the detectable fraction remained largely unchanged.

Although a digestion temperature of 25°C resulted in slightly lower mean values for particle number and mass concentration recoveries, these differences are not statistically significant. Based on these results, incubation of Eu-PS-NPs in citrate buffer at pH 6.5 and 37°C was selected as the optimal conditions.

### 3.2.2. *Optimization of the post-digestion stage*

To separate the extracted Eu-PS-NPs from residual plant debris following digestion, the digested spiked root samples were subjected to 30 min settling or centrifugation at varying durations and speeds as described in Section 2.3. Recovery values for all treatment groups are depicted in Fig. 1b and detailed in Table S5. The centrifugation at 1000 or 2000 rpm for 3 or 5 min exhibited similarly high recoveries for particle number (112 – 117 %) and mass concentration (110 –111 %). All these treatment groups displayed similar recoveries to the control group (no centrifugation with 30 min settling time). In all treatment groups, the recoveries for median particle diameter (98 – 99 %) and median particle mass (94 – 97 %) remained stable and comparable, thereby demonstrating no effect of centrifugation on particle size and mass. Based on the data, all subsequent analyses applied a 30 min post-digestion settling step.

### 3.2.3. *Optimization of digestion time and enzyme concentration*

To evaluate the impact of digestion time (24 h *vs.* 36 h) and enzyme concentration (10, 50, 100 mg of enzyme per 25 mg of sample) on the extraction of Eu-PS-NPs from tomato tissue, spiked root, stem, leaf, and fruit samples were prepared and treated as described in Section 2.3. The results are given in Table S6 and graphically presented in Fig. 2.

**Roots:** 24 h digestion of the spiked root samples with 10 mg enzyme/sample resulted in a particle number concentration recovery of 103.5 ± 4.6 %, and particle mass concentration recovery of 94.8 ± 3.7 %. While increasing enzyme concentration had minimal effect on the recoveries, with no statistically significant differences observed, extending the digestion time to 36 h improved both particle number and mass concentration recoveries. After 36 h of digestion, the particle number and mass concentration recoveries increased compared to 24 h, reaching 114.0 ± 10.3 % and 112.5 ± 7.6 % at 10 mg enzyme/sample, respectively. With longer digestion times, recoveries for median particle diameter (98 %) and particle mass (95 %) improved compared to 24 h digestion. Higher recoveries at 36 h suggest that extended enzyme

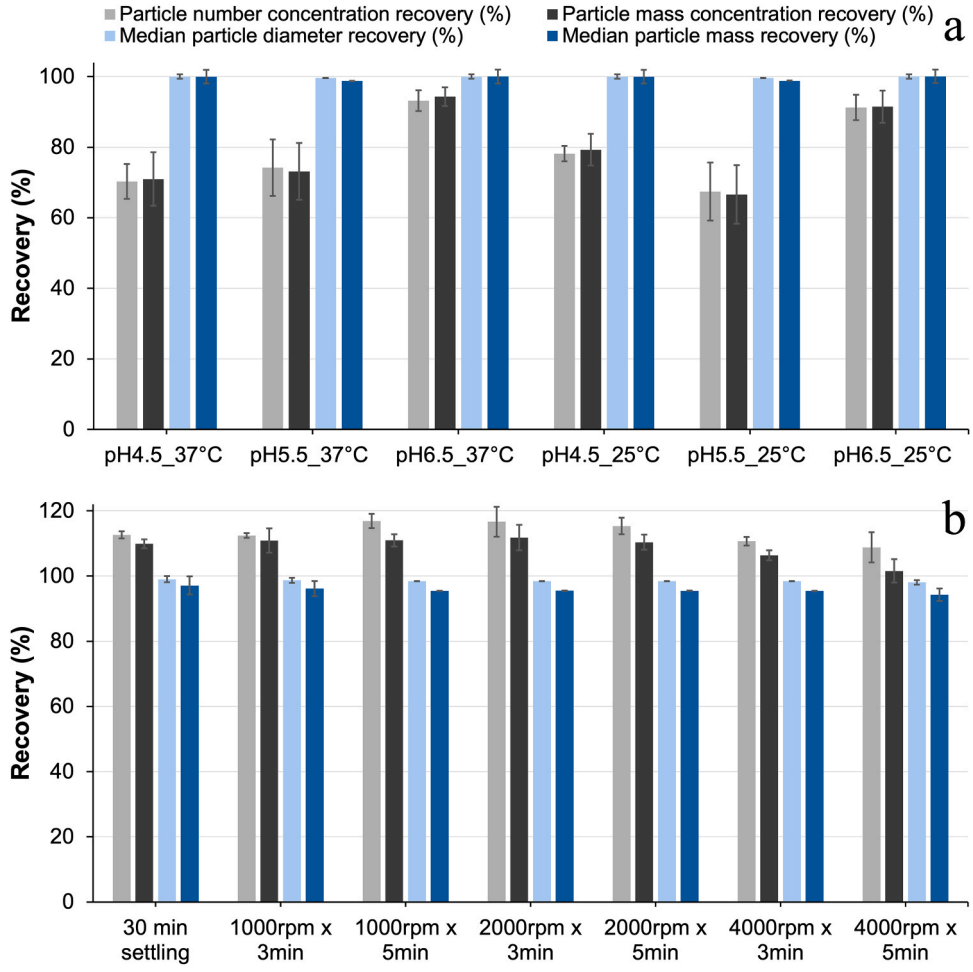


**Fig. 1.** Eu-PS-NPs recoveries for different citrate buffer pH and digestion temperatures (a), and different post-digestion conditions (b). Results are given as mean ± STD (N = 3). rpm = revolutions per minute; min = min.

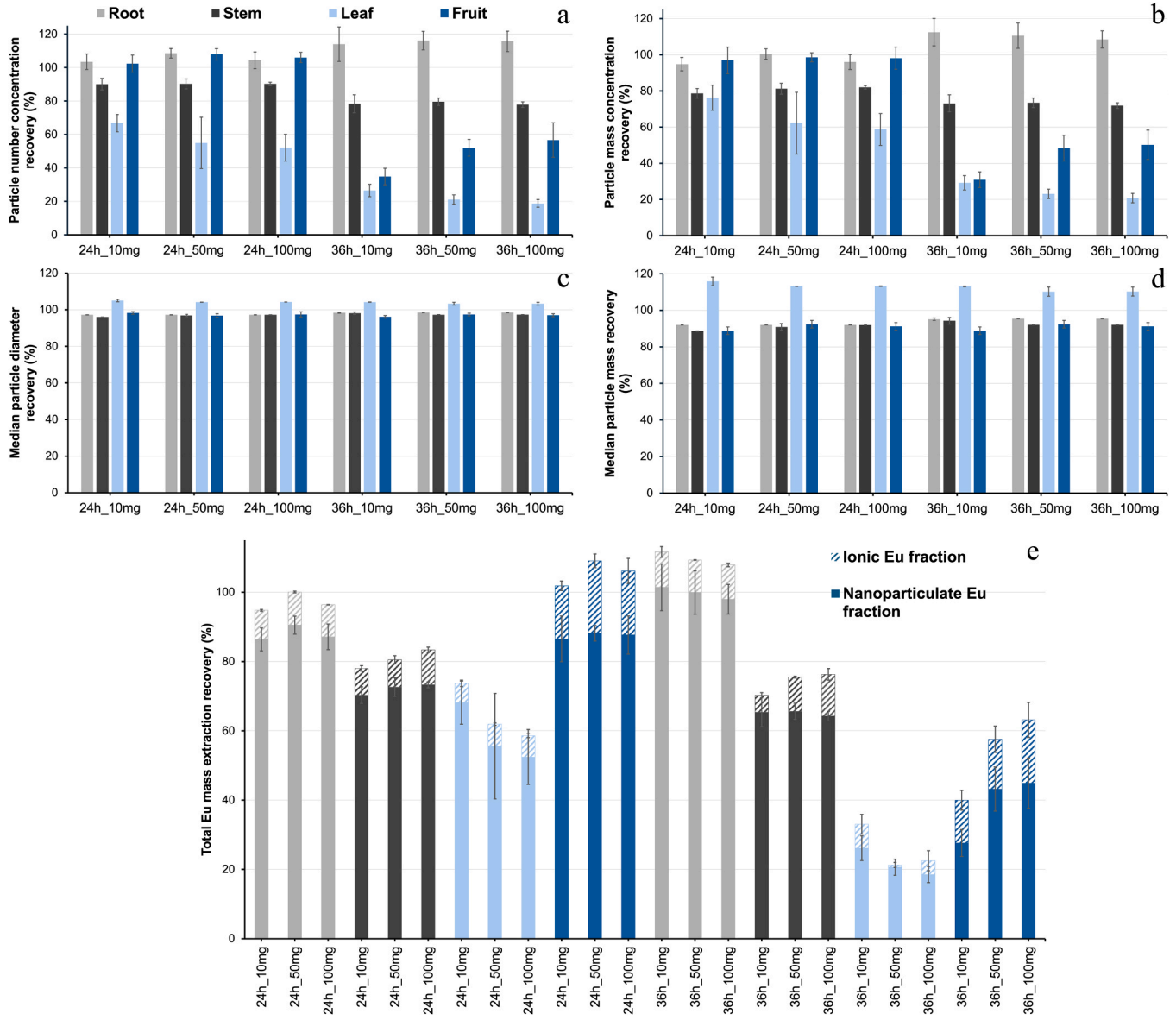


**Fig. 2.** Extraction recoveries of Eu-PS-NPs from spiked tomato tissues following enzymatic digestion under varying enzyme concentrations and digestion durations. Bars represent mean ± STD (N = 3) for: (a) particle number concentration recovery, (b) particle mass concentration recovery, (c) median particle diameter recovery, (d) median particle mass recovery, (e) total Eu mass extraction recovery with relative contributions of nanoparticulate and ionic Eu forms. h = h; mg = milligrams.

exposure more effectively liberates or stabilizes NPs from the root matrix. Interestingly, increasing enzyme concentration did not significantly improve recoveries, suggesting that extraction efficiency reaches a threshold, beyond which further enzyme addition offers no added benefits.

**Stems:** A 24 h digestion of spiked stem samples using 10 mg enzyme/sample resulted in recoveries of 90.0 ± 3.5 % for particle number concentration and 78.7 ± 2.7 % for particle mass concentration. Increasing the enzyme concentration did not result in significant improvements in particle recoveries. After 36 h of digestion, particle number (78.3 ± 5.4 %) and mass concentration recovery (73.2 ± 4.7 %) decreased when using 10 mg enzyme/sample. The median particle diameter recoveries remained consistent across treatment groups, ranging from 96.1 % to 98.1 %, indicating that the digestion process had minimal impact on particle shape. In contrast to spiked root samples, spiked stem samples showed reduced recoveries with extended digestion, implying that optimal extraction conditions differ significantly between stems and roots. Macerozyme R-10 is primarily a pectinase enzyme used for cell wall digestion. Root cell walls, particularly in the epidermis, contain significant amounts of pectin in the middle lamella (Chialva et al., 2019), whereas stems have more cellulose- and lignin-rich secondary walls (Dahal et al., 2010), which could explain the lower extraction recovery in stems compared to roots.

**Leaves:** A 24 h digestion of spiked leaf samples using 10 mg enzyme/sample resulted in recoveries of 66.7 ± 5.2 % for particle number concentration and 76.3 ± 7.0 % for particle mass concentration. Increasing the enzyme concentration resulted in recovery losses of up to 18 %, while prolonged digestion (36 h) led to an even more pronounced decrease in recoveries by as much as 47 %. For instance, 36 h digestion with 10 mg enzyme/sample yielded a particle number concentration recovery of 26.5 ± 3.7 %, which decreased to 18.8 ± 2.3 % with 100 mg enzyme/sample. The median particle diameter and mass recoveries remained relatively stable and consistently high across all treatment groups, ranging from 103.3 % to 105.0 % and from 110.2 % to 115.8 %, respectively, suggesting the formation of larger particle aggregates during extraction. Significantly lower extraction recoveries observed in leaves compared to roots and stems could be explained by the variations in anatomical structure across different tomato parts. Leaf

surfaces contain very-long-chain aliphatics (VLCAs) and triterpenoids that form a highly hydrophobic barrier, which could render the leaf tissue resistant to enzymatic degradation (Seufert et al., 2022). The lipophilic surface of NPs will have a strong affinity with the leaf wax layer, potentially causing them to embed within this matrix rather than being released during enzymatic digestion (Zhou and Xia, 2024).

Moreover, the observed pattern of decreasing NPs extraction recovery with prolonged digestion in spiked tomato stems and leaves, contrasted with increasing recovery in spiked roots with time, strongly suggests tissue-specific interactions between NPs and plant compounds released during enzymatic extraction. Tomato plants exhibit significant variation in phenolic compound distribution across different tissues: leaves contain the highest diversity and levels of phenolic compounds, particularly flavonoids and hydroxycinnamic acids; stems possess intermediate levels of phenolics, with distinct composition profiles compared to leaves, while roots exhibit the lowest phenolic content among the three tissue types, with minimal flavonoid accumulation (Larbat et al., 2014; Silva-Beltrán et al., 2015). The primary mechanism responsible for decreased NPs extraction recovery with increased time in leaf and stem tissues likely involves polyphenol-mediated coagulation of NPs during the extraction. These interactions become more pronounced with prolonged digestion as more polyphenols are released from cellular compartments, explaining the progressive decrease in NPs recovery from leaf and stem tissues. Interestingly, this phenomenon has been previously reported and studied as an efficient strategy for MPs removal from water samples through metal-phenolic bonding, leading to their coagulation and settlement (Park). It should be noted that the metal–phenol coagulation mechanism has not yet been investigated in detail and is currently proposed as a working hypothesis to explain the observed recovery losses.

**Fruits:** A 24 h digestion of the spiked fruit samples with 10 mg enzyme/sample yielded recoveries of 102.3 ± 5.1 % for particle number concentration and 96.9 ± 7.4 % for particle mass concentration. While increasing enzyme concentration had minimal effect on recoveries, with no significant differences observed, extending the digestion time to 36 h significantly reduced recoveries. Following 36 h of digestion with 10 mg enzyme/sample, particle number concentration recovery dropped to 34.9 ± 5.00 %, and particle mass concentration recovery to 30.9 ± 4.4 %. The reduction in extraction recoveries observed with prolonged digestion time could be attributed to the destabilization of NPs under their extended exposure to acidic conditions. A low pH likely promoted NPs aggregation, as indicated by the increase in hydrodynamic diameter and the reduction in negative surface charge with decreasing pH (Section 3.1), ultimately leading to particle loss, as evidenced by the decrease in particle number and mass concentration recoveries under lower pH conditions (Section 3.2.1). Specifically, tomato fruits are naturally acidic, primarily due to the presence of organic acids such as citric and malic acids (Agius et al., 2018), particularly concentrated in the pericarp and locular tissues (Mahakun et al., 1979). Increasing enzyme concentrations led to improved yet still low recoveries (56.7 % for particle number concentration and 50.3 % for particle mass concentration when using 100 mg enzyme/sample). The median particle diameter and mass recoveries were relatively stable across all treatment groups, ranging from 96.1 % to 98.2 % and from 88.8 % to 92.4 %, respectively, indicating that digestion maintains particle diameter.

Maintaining minimal or well-controlled Eu leaching throughout the analytical procedure is crucial for the reliable use of Eu as a proxy for NP detection via spICP-MS. To assess potential Eu leaching during enzymatic digestion, we quantified Eu associated with both nanoparticulate and ionic forms by spICP-MS, expressing them as mass fractions of the total Eu mass concentration (Fig. 2e). The mass fraction of ionic Eu relative to the total Eu mass concentration was not affected by the enzymatic extraction and was comparable to that observed in the Eu-PS-NPs water suspension (10.5 ± 0.3 %, Section 3.1), ranging from 8 to 10 % in spiked roots, 10 –12 % in spiked leaves, and 11–14 % in spiked stems. Compared to the standard solution, only the spiked fruit sample had a significantly higher mass fraction of ionic Eu detected (*t*-test, $p < 0.05$), ranging between 17 % after 24 h and 28 % after 36 h of digestion. The elevated mass fraction of ionic Eu in the presence of the fruit matrix is likely due to its acidic nature, which promotes Eu leaching from NPs.

#### 3.2.4. *Effect of drying temperature on the extraction efficiency*

Before enzymatic extraction and subsequent spICP-MS analysis, exposed tomato samples were first dried at 60°C for 48 h and then ground using liquid nitrogen (Section 2.2). Oven-drying of plant tissues at 60 °C was selected as a simple and widely established method that efficiently removes moisture while preserving plant matrix integrity, with the temperature remaining well below the glass transition temperature of polystyrene (80–105 °C) and the melting range of its crystalline phases (240 –270 °C).

The influence of 60°C on the Eu-PS-NP morphology was studied using SEM, and compared to the Eu-PS-NPs exposed to 25°C. The Eu-PS-NPs imaged after 48 h exposure to 25°C were spherical, of uniform size and shape and did not exhibit any deformations and/or aggregations (Fig. 3a). Alternatively, after exposure to 60°C, Eu-PS-NPs predominantly retained their spherical morphology but exhibited slight deformations, including signs of melting and aggregation, with particles adhering to one another. These observations suggest that a drying temperature of 60°C is likely to affect the integrity of the Eu-PS-NPs in the exposed tomatoes and, consequently, influence the ability to extract them from the samples effectively.

To test this hypothesis, separate batch experiments were conducted to assess the effect of 60°C on Eu-PS-NPs extraction recoveries, in which control tomato samples were spiked with Eu-PS-NPs and exposed to either 25°C or 60°C for 48 h. A significant reduction in particle number and mass concentrations, as well as total Eu mass concentration, was observed in the spiked samples exposed to 60°C for all tomato tissues (Figure S1). The extent of loss varied among different tomato parts, with the greatest decrease observed in roots (around 65 %) and the least in stems (approx. 27 %). Exposure of leaf samples to 60°C led to reductions in particle diameter and mass, whereas no significant changes were observed in particle size for other tomato tissues. Furthermore, the drying step resulted in only a minimal increase in ionic Eu (0.3 % increase observed in roots and up to 6.2 % increase in fruit), suggesting a negligible impact of sample drying on Eu leaching. Taking these results into account, correction factors were calculated for each tomato part (Table S7) to compensate for particle loss caused by the prior exposure of tomato samples to 60°C during the drying step. It should also be noted that the brief cryogenic grinding step in liquid nitrogen applied to plant samples after drying may affect the physical state of PS NPs. The standard's manufacturer advises against prolonged exposure to freezing temperatures, as this may induce their irreversible aggregation; however, the potential impact of this step on NPs extraction efficiency from plant tissue was not assessed in the present study.

### 3.3. *Evaluation of enzymatic extraction parameters for the analysis of Eu-PS-NPs accumulated in exposed tomato samples*

The enzymatic extraction procedure was further tested on tomatoes exposed to Eu-PS-NPs. The distinction between spiked and exposed samples is important, as extraction from spiked samples targets externally introduced Eu-PS-NPs, allowing assessment of how digestion parameters and matrix composition affect NPs stability and recoveries. In contrast, extraction from exposed tomato samples requires isolation of internally accumulated particles through the digestion of the plant matrix, providing a measure of the actual efficacy of the extraction process. Notably, whereas most published studies have relied on spiked samples alone to demonstrate the efficacy of the digestion procedures, distinguishing between spiked and exposed tomato samples, our study facilitates a more objective assessment of the extraction protocol under

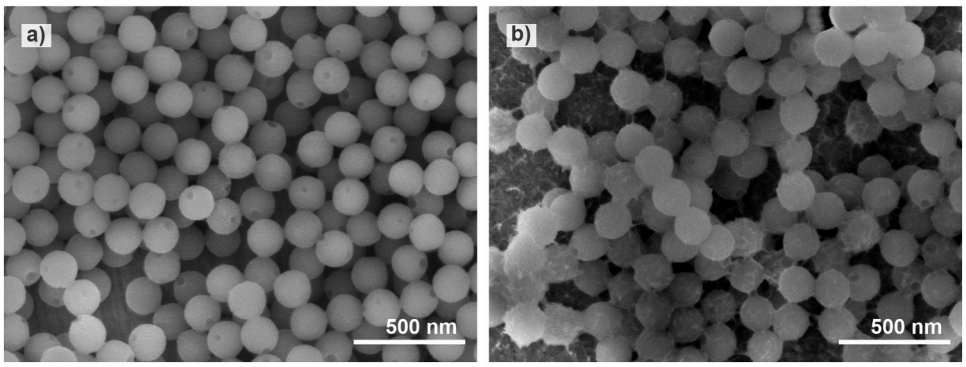


**Fig. 3.** SEM analysis of Eu-PS-NPs exposed to 25°C (a) and 60°C (b) for 48 h. nm = nanometers.

controlled and biologically relevant conditions, while also highlighting key differences in recovery behaviour.

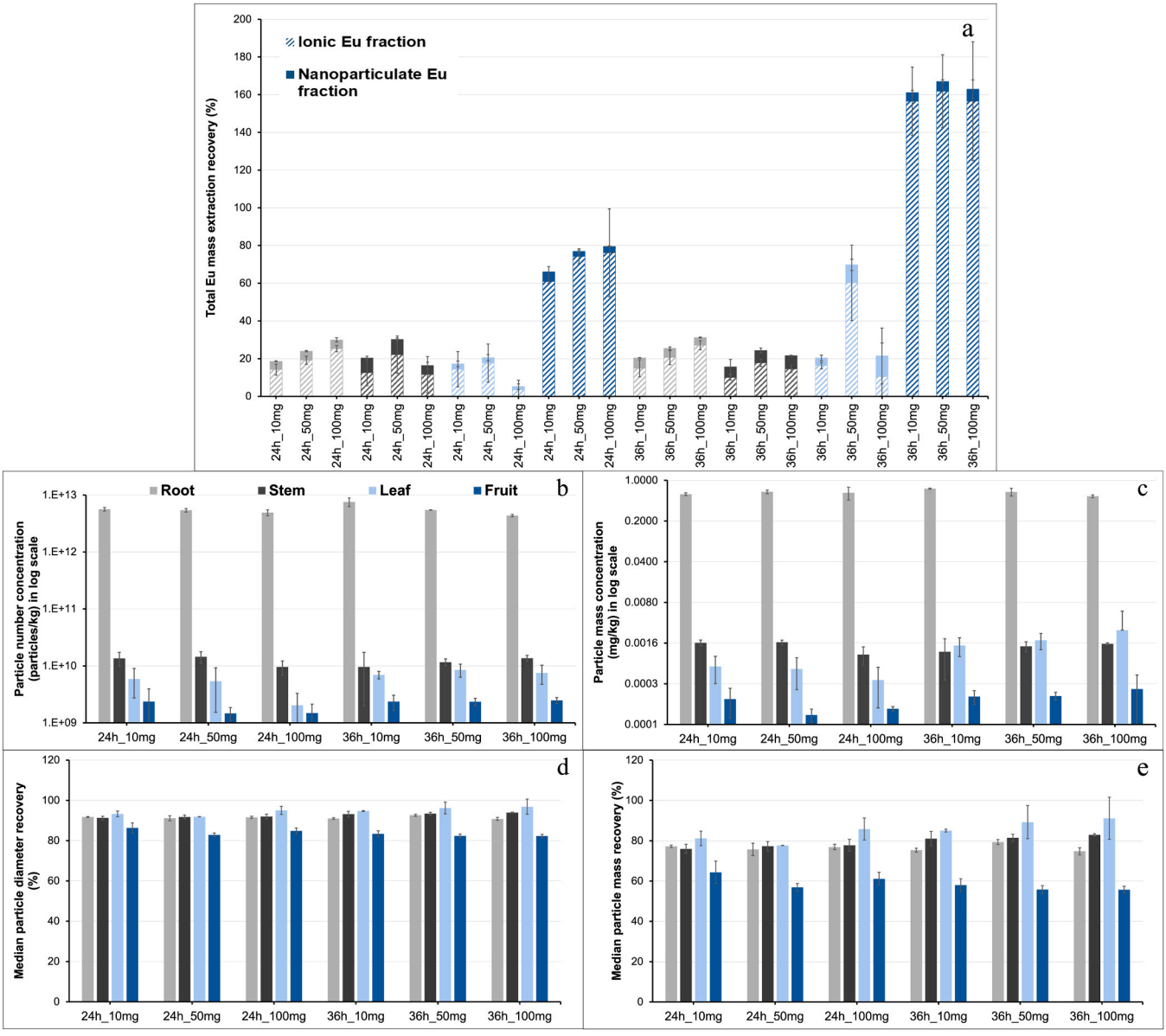


**Fig. 4.** Results for Eu-PS-NPs extracted from exposed tomato samples following enzymatic digestion under varying enzyme concentrations and digestion durations. Bars represent mean ± STD (N = 3) for: (a) total Eu mass extraction recovery with relative contributions of nanoparticulate and ionic Eu forms, (b) particle number concentration, (c) particle mass concentration, (d) median particle diameter recovery, and (e) median particle mass recovery. Data have been corrected using the drying loss factors and matrix-specific recovery factors determined from spiked samples. h = h; mg = milligrams.

*3.3.1. Impact of digestion time and enzyme concentration on extraction efficiency*

To calculate the total Eu mass extraction recovery from exposed tomatoes, another correction factor was introduced in addition to the one accounting for particle loss due to drying at 60°C (see Section 3.2.4). This second correction factor, specific to each tomato part and derived from the recoveries of spiked samples (Table S7), accounts for any matrix-specific or procedural losses observed during the extraction from the spiked samples.

Total Eu mass extraction recoveries varied depending on tissue type, digestion time, and enzyme concentration used (Fig. 4a). In the case of root samples, 24 h digestions using 10, 50, and 100 mg enzyme/sample resulted in recoveries of 18.6 ± 3.1 %, 24.0 ± 2.3 %, and 29.9 ± 2.0 %, respectively, with slight increase observed when extending the digestion time to 36 h. For stem samples, the highest recovery of 30.2 ± 10.0 % was achieved with 50 mg enzyme/sample after 24 h digestion, whereas both lower and higher enzyme concentrations, as well as prolonged digestion to 36 h resulted in lower recoveries. For leaf samples, 24 h digestion with 10 mg enzyme/sample resulted in a recovery of 17.3 ± 10.1 %, which further decreased to 5.2 ± 6.1 % as the enzyme concentration increased. However, 36 h digestion at 50 mg enzyme/sample significantly improved recovery to 69.8 ± 22.8 %, which may be influenced by an outlier sample, as the bioaccumulation of NPs in plants is known to be heterogeneous and typically follows a clustered distribution pattern (Sahai et al., 2024). Fruit samples showed high apparent recoveries already after 24 h of digestion (ranging from 66.1 ± 3.5 % to 79.6 ± 23.6 %). However, after 36 h, the recoveries exceeded 160 % across all enzyme concentrations. This anomaly may be explained by the results from spiked fruit samples, where recoveries reduced by half after 36 h (40 – 60 %) as opposed to 24 h (100 – 110 %, see Fig. 2). When these reduced recoveries are used to calculate correction factors for total Eu mass extraction recoveries, they can result in recoveries in exposed fruits exceeding 100 %. Given that nearly 100 % recovery was achieved in spiked fruit samples after 24 h, prolonged digestion (36 h) appears unnecessary for fruit.

This discrepancy between the high recoveries observed in spiked samples and the lower recoveries in exposed samples is likely attributable to differences in NP localization within the plant matrix. In spiked samples, NPs are predominantly associated with the surface of the biomass, making them readily accessible to enzymatic digestion and subsequent release. In contrast, in exposed samples, NPs are biologically incorporated into plant tissues, where they may become potentially trapped within complex lignocellulosic structures or intracellular compartments. Two possible mechanisms may account for the reduced recoveries in exposed samples. First, a fraction of the NPs may remain associated with undigested plant residues that are removed during the post-digestion settling step. This suggests that, although enzymatic digestion partially disrupts the plant matrix, it may be insufficient to fully liberate particles embedded within recalcitrant structural components. In this context, repeated or sequential extraction steps could be explored to improve particle release. Second, the enzymatic activity of Macerozyme R-10 alone may be inadequate to achieve complete tissue digestion. It is therefore important to emphasize that these data represent only the extractable fraction of Eu–PS NPs and thus likely underestimate the total amount of Eu–PS NPs bioaccumulated in the exposed tomato tissues. Future work should therefore investigate alternative alkaline treatments using TMAH, which has been shown to efficiently release NPs from biological tissues (Li et al., 2021b, 2023; Lai et al., 2025), or complementary enzyme systems, including combinations of *cellulases*, *hemicellulases*, lignin-degrading enzymes, and *proteases* (e.g., proteinase K), to enhance matrix degradation and improve nanoparticle extraction efficiency. It is also important to note that the recovery values reported here refer to total Eu mass concentration, which includes nanoparticulate-associated Eu fraction, representing intact Eu-PS-NPs, and ionic Eu fraction present in the sample as a result of Eu leaching from NPs. Calculating mass fraction of ionic Eu in the extracts of exposed tomato samples revealed that the vast majority of Eu detected was present in ionic form, with only a minor and highly treatment-dependent fraction remaining associated with intact NPs (Fig. 4a). In root samples, the ionic Eu fraction ranged from 75.8 ± 3.1 % after 24 h of digestion with 10 mg enzyme/sample to 86.8 ± 1.4 % after 36 h with 100 mg enzyme/sample. Stem samples showed the lowest ionic Eu fraction after 24 h with 10 mg enzyme/sample (58.5 ± 11.3 %), which increased to 72.9 ± 3.2 % after 36 h with 50 mg enzyme/sample. Leaf samples exhibited variable ionic Eu fraction, ranging from 71.6 ± 35.4 % (24 h with 100 mg enzyme/sample) to 86.2 ± 1.3 % (36 h with 50 mg enzyme/sample). In fruit extracts, the ionic Eu fraction dominated, accounting for 92.3 ± 3.7 % after 24 h with 10 mg enzyme/sample, and increasing to 97.1 ± 0.9 % after 36 h with the same enzyme concentration, leaving less than 7.7 ± 3.7 % of Eu associated with intact particles. Neither enzymatic treatment itself nor sample drying at 60 °C significantly contributed to the leaching of ionic Eu from Eu-PS-NPs, as observed in spiked samples (Sections 3.2.3 and 3.2.4). Instead, the significant presence of ionic Eu in exposed tomato samples likely results from the leaching of bioaccumulated Eu-PS-NPs within the tissue during plant exposure, further influenced by the tomato matrix. One of the tissue-specific factors that may influence Eu leaching is pH. A moderate inverse correlation was observed between the pH values of extracts from exposed tomatoes (Table S9) and the ionic Eu mass fraction ($r = -0.52$), suggesting that lower pH might contribute to Eu leaching, although it is not the only influencing driver. Eu(III) chelates (e.g., Eu-NTA, β-diketonates) exhibit optimal stability at pH 6–8 but protonate and release free $Eu^{3+}$ below pH 5 due to competition from $H^+$ ions (Kokko et al., 2007). Finally, a multifactor ANOVA, including factors such as tissue type, digestion time, enzyme concentration, and pH, revealed that tissue type alone accounted for more than 70 % of the explained variance in ionic Eu mass fractions ($SS = 1.393$; $F = 17.6$; $p < 0.0001$). It is, however, important to keep in mind that this tissue-specific variance itself is a result of different compositional profiles and tissue pH. Furthermore, the substantial leaching observed in our samples can be attributed to the architecture of NPs employed in this study. As described in Section 2.1, the particles used here are manufactured such that metal tracer is present as an organic chelate dispersed within the PS matrix and enriched toward the particle periphery, where carboxyl groups are located, effectively yielding a PS core with an Eu-rich outer layer (Liang et al., 2015). Particle integrity can be further verified using scanning or transmission electron microscopy (STEM) coupled with energy-dispersive X-ray spectroscopy (EDS) to reveal the spatial distribution of Eu, or by monitoring fluorescence quenching of Eu-chelates, which serves as an in-situ indicator of label dissociation (Weissman, 1942). This structural arrangement leaves the Eu chelate relatively exposed and susceptible to protonation under acidic conditions (Kokko et al., 2007), which can promote dissociation and leaching in biological environments, such as the acidic tissues of tomato fruits. These findings indicate that NPs labelled in this manner are not suitable as quantitative tracers in acidic biological matrices or for long-term exposure experiments, as the metal signal may no longer reliably represent the polymer particle. To avoid desorption, an alternative and more robust approach is the fabrication of an MNP containing an entrapped metal in a core–shell structure. In such designs, a metal-rich core is fully encapsulated within a polymer shell, preventing direct interaction between the metal and the surrounding environment (Mitrano et al., 2019). This configuration enables higher metal loading per particle and has been shown to exhibit minimal leaching in water and simple media (Crosset-Perrotin et al., 2025). Nevertheless, the possibility of metal leaching from core–shell NPs within complex plant tissues has not yet been conclusively excluded. Given that plant and food matrices are often acidic and rich in organic ligands, optimal tracer designs would ideally involve deeply encapsulated labels—for example, europium complexes covalently fixed within a silica core and protected by an outer polymer shell—or be complemented by polymer-specific analytical techniques, such as pyrolysis-GC-MS, to independently verify NP fate.

The absolute values for particle number concentration (particles/kg) extracted from exposed tomato samples also exhibited tissue-specific responses to enzyme concentrations and digestion times (Fig. 4b). In root samples, a 24 h digestion with 10 mg enzyme/sample yielded the highest particle number concentration of $5.64 \times 10^{12} \pm 4.12 \times 10^{11}$ particles/kg, which declined with increasing enzyme concentration. Extending the digestion to 36 h at the same enzyme concentration further increased the particle number concentration to $7.58 \times 10^{12} \pm 1.33 \times 10^{12}$ particles/kg, while higher enzyme concentrations also led to a reduction in particle number. In stem samples, the particle number concentration after 24 h of digestion with 10 mg enzyme/sample was $1.35 \times 10^{10} \pm 3.76 \times 10^{9}$, with no significant changes observed upon extending the digestion time or increasing the enzyme concentrations. The particle number concentration extracted from exposed leaf samples showed a time-dependent trend, ranging from 2.04 to $5.90 \times 10^{9}$ particles/kg after 24 h of digestion and increasing to $6.96–8.53 \times 10^{9}$ particles/kg after 36 h, suggesting that extended digestion can help mitigate enzyme-induced particle loss in waxy or cuticle-rich leaf matrices. In fruit samples, particle number concentrations were uniformly low ($1.47–2.48 \times 10^{9}$ particles/kg), with no significant variation observed across different enzyme concentrations or digestion durations. The particle mass concentrations of Eu-PS-NPs extracted from exposed tomato samples exhibited similar trends to those observed in particle number concentrations, with tissue-specific variations in response to enzyme concentrations and digestion times (Fig. 4c).

Moreover, the median particle diameters and median particle masses of the extracted Eu-PS-NPs were compared to those of the Eu-PS-NPs aqueous suspension (Fig. 4d and e). In root samples, median diameters ranged from 90.8 % to 92.6 % across all enzyme concentrations and digestion times, with corresponding median particle masses between 74.8 % and 79.4 % of the standard. Similarly, NPs extracted from stem samples exhibited median particle diameters ranging from 91.3 % (after 24 h with 10 mg enzyme/sample) to 94.0 % (after 36 h with 100 mg enzyme/sample), with corresponding median particle mass recoveries between 76.0 % and 82.9 %. Furthermore, leaf samples contained particles with median particle diameters spanning from 91.9 % (24 h with 50 mg enzyme/sample) up to 96.9 % (36 h with 100 mg enzyme/sample) and median particle masses ranging from 77.7 % to 91.1 %. In contrast, particles extracted from exposed fruit samples exhibited the most pronounced reduction in both median particle diameter and mass. Median diameter decreased from 86.3 % (after 24 h with 10 mg enzyme/sample) to as low as 82.3 % following 36 h digestion with 50 mg enzyme/sample. Similarly, median particle masses decreased from 64.4 % to 55.8 %. Particle sizes detected in both spiked and exposed tomatoes were smaller than those in the standard solutions, with a more pronounced reduction in the exposed samples (Fig. 5), indicating a stronger impact on particle integrity during bioaccumulation in tomato tissues. This reduction may be attributed to the partial leaching of Eu from the chelated PS-NPs, leading to decreased particle signal intensity in spICP-MS measurements and, consequently, smaller calculated particle mass and diameter. A Pearson's correlation analysis between the median particle diameter and mass fraction of ionic Eu reveals a moderate negative correlation, with a coefficient of −0.71. Similarly, a coefficient of −0.69 is observed between the median particle mass and the ionic Eu fraction, demonstrating that the leaching of Eu from Eu-PS-NPs is moderately responsible for the reduction in both particle mass and diameter observed in exposed tomato samples. The reduction in particle size and mass was particularly notable in exposed fruit samples (Fig. 5d), further confirming the increased Eu leaching from NPs in this tissue, most likely due to the acidic nature of the fruit matrix. Furthermore, exposed samples exhibited a greater number of larger particles compared to both standard Eu-PS-NPs and those extracted from spiked samples, further highlighting the heterogeneous nature of NPs bioaccumulation in plants, which typically follows a clustered distribution pattern.

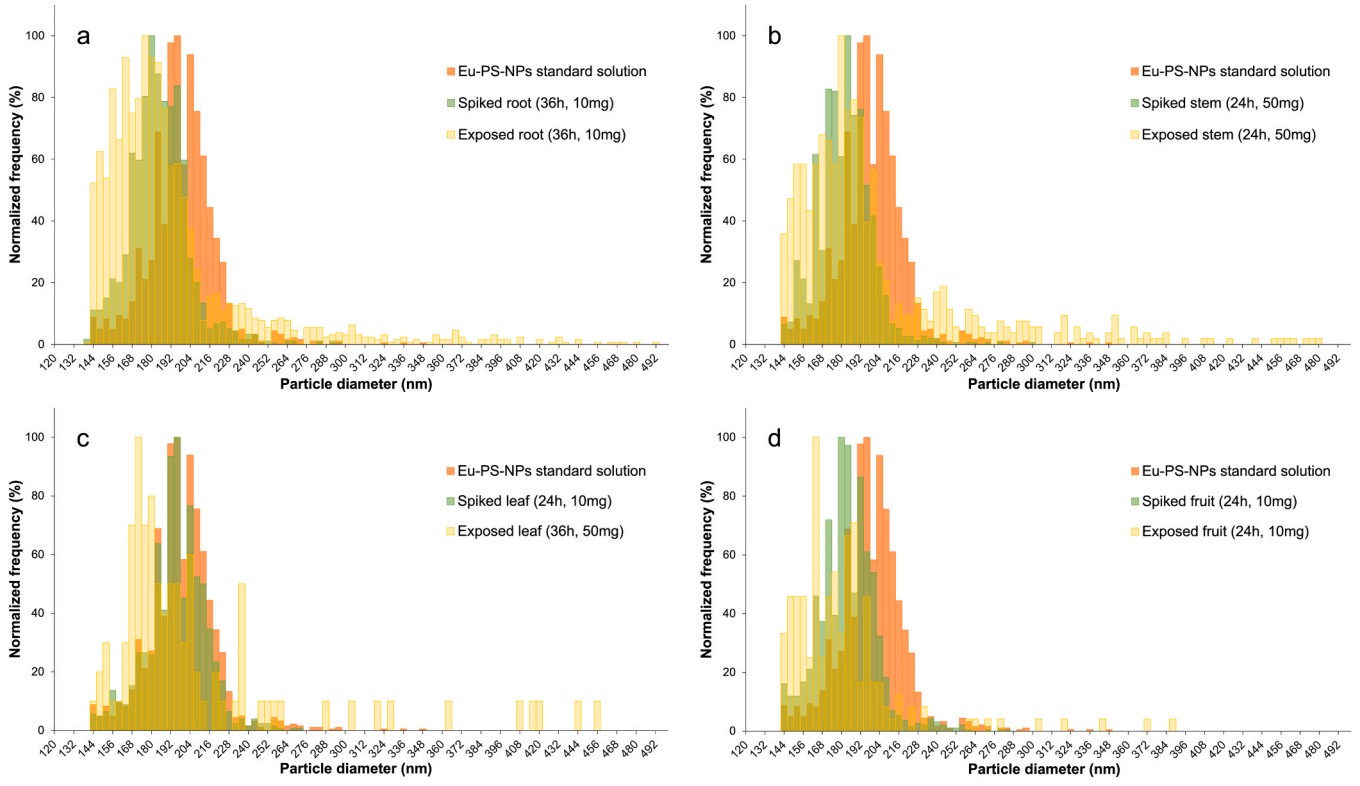


**Fig. 5.** Number-based particle size distribution of Eu-PS-NPs extracted from spiked and exposed tomato samples, compared to the particle size distribution of Eu-PS-NPs standards prepared in water solution. Distributions in roots (a), stems (b), leaves (c), and fruits (d) were obtained under optimized extraction conditions. h = h; mg = milligrams; nm = nanometers.

*3.3.2. Effect of post-digestion pH adjustment on the extraction efficiency*

The pH of the extraction medium can influence the stability of the Eu-PS-NP (Sections 3.1 and 3.2.1), which ultimately affects their recovery. For instance, the pH of extracts from exposed tomato samples varied noticeably depending on enzyme concentration and digestion time across different tomato tissues (Table S9). Increasing enzyme concentration led to a drop in pH, with the most significant changes observed in root and leaf samples. For example, in root tissue, the pH decreased from 6.24 at 10 mg enzyme/sample to 5.47 at 100 mg enzyme/sample after 24 h digestion, while in leaves, it reduced from 6.61 to 4.80 under the same conditions. Fruit samples also exhibited lower pH values across all treatments (pH 4.94–4.86), likely due to their naturally higher acidity. These findings suggest that, in addition to the selected citrate buffer pH, enzyme concentration significantly affects the pH environment during digestion, which in turn may impact the effectiveness of NPs recovery from different tomato tissues. To test this hypothesis, exposed tomato samples were subjected to an additional post-digestion pH adjustment step, where the pH of the digested samples was adjusted to 7.0 ± 0.2 before collection of the supernatant. Overall, pH adjustment had no significant impact on the extraction of Eu-PS-NPs compared to non-adjusted samples (Tables S10 and S11). In some treatment groups, recovery was even reduced. Although slight improvements were observed in some instances (e.g., fruit samples), these increases were not statistically significant due to intra-replicate variability.

All previously reported recoveries were obtained from samples extracted using a citrate buffer at pH 6.5, selected based on the optimal pH for NPs stability (Section 3.2.1), despite the optimal activity of Macerozyme R-10 being reported at pH 4.0. To evaluate whether the starting pH limited plant digestion efficiency and contributed to lower extraction recoveries of Eu-PS-NPs from exposed tomato samples, additional exposed stem samples were digested using citrate buffer at pH 4.5 and analyzed by spICP-MS. Adjusting the citrate buffer pH to 4.5 did not enhance the extraction efficiency; instead, it resulted in a significant decrease in the particle number and mass concentration of Eu-PS-NPs recovered from the exposed stem samples compared to those extracted with citrate buffer at pH 6.5 (Table S12).

## 4. Conclusions

This study provides valuable methodological insights into the analysis of metal-labelled NPs in plants, importantly contributing to advancing the understanding of plant exposure and responses to NPs. As more evidence emerges demonstrating the bioaccumulation of MNPs in plants, it becomes imperative that suitable analytical methodologies are developed capable of performing selective, sensitive, and quantitative analysis of NPs inside plant tissues. This study presents an analytical procedure for quantifying Eu-labelled PS NPs in different tomato tissues, combining enzymatic extraction with spICP-MS analysis. Systematic optimization of the extraction conditions using spiked tomato samples revealed that optimal extraction conditions are highly tissue-specific, and that prolonged digestion times or higher enzyme concentrations generally do not improve extraction efficiency. The extraction of Eu-PS-NPs from exposed tomato samples was also highly tissue-specific, with total Eu mass recoveries significantly lower than those observed in spiked samples. In spiked samples, most Eu was associated with NPs, with only about 10 % present as ionic Eu, comparable to the standard Eu-PS-NPs suspension, whereas in exposed tomato samples, Eu was mainly ionic (up to 97 % in fruits), indicating extensive leaching within the plant, while digestion parameters had minimal impact.

These differences between spiked and exposed tomato samples highlight two critical considerations for quantitative spICP-MS analysis of metal-labelled NPs bioaccumulated in plants. First, extraction recoveries based on the evaluation of total Eu mass concentration and derived solely from spiked control samples can misrepresent actual extraction efficiency from exposed tomato tissues. Evaluation of ionic Eu content and matrix-specific correction factors is therefore essential for reliable interpretation of the results. Second, these results highlight the importance of developing metal tracers for NPs that remain embedded within the polymer matrix and stable within plant tissue, ensuring their reliable use as digestion protocols require a balance between achieving complete tissue breakdown while preserving NPs' integrity. Particle architectures such as those employed in this study, in which the Eu chelate is embedded within the polymer matrix but preferentially enriched in an outer shell, are susceptible to substantial tracer leaching when exposed to acidic biological matrices over extended periods. This susceptibility limits their suitability for quantitative applications under such conditions. Future studies should therefore investigate more robust tracer designs, such as covalently bound labels or well-defined core–shell lanthanide architectures, to enhance tracer stability. Single-particle ICP-MS remains a powerful analytical technique, as it provides number-based particle concentrations and size information with very low detection limits. However, complementary polymer-specific methods, such as pyrolysis GC–MS, can be used to quantify the nanoplastic itself, acknowledging that it lacks direct information on particle size or number, and is therefore best applied alongside particle-resolved approaches such as asymmetric flow field-flow fractionation (AF4) or nanoparticle tracking analysis (NTA). Future research should explore alkaline treatment or alternative enzyme combinations, such as mixtures of *cellulase, hemicellulase, ligninase, proteinase-K*, or other *proteases*, in an attempt to enhance extraction efficiency, as well as prioritize tissue-specific extraction protocols, accounting for variations in anatomical structure, biochemical composition, hydration level, and nanoparticle–matrix interactions. It should be noted that the uptake and tissue distribution patterns reported here are specific to Eu-PS NPs with the particular size and surface chemistry employed in this study, and should not be directly extrapolated to uncoated or differently functionalized PS nanoparticles, which may exhibit substantially different aggregation behaviours and bioreactivities. Future investigations should include comparative studies of other metal-doped, uncoated, and alternatively surface-modified PS NPs (including both metal- and organic-functionalized variants) to distinguish effects attributable to the tracer from those inherent to the polymer itself.

## CRediT authorship contribution statement

**Harshit Sahai:** Writing – original draft, Visualization, Methodology, Investigation, Formal analysis, Data curation, Conceptualization. **María Jesús Martinez Bueno:** Writing – review & editing, Funding acquisition. **Janja Vidmar:** Writing – review & editing, Supervision, Project administration, Investigation, Formal analysis, Data curation, Conceptualization. **Nina Kacjan Maršić:** Writing – review & editing, Resources. **Špela Železnikar:** Writing – review & editing, Resources. **Matejka Podlogar:** Writing – review & editing, Visualization, Formal analysis. **Tina Radošević:** Writing – review & editing, Visualization, Formal analysis. **Pia Leban:** Writing – review & editing, Methodology. **Ester Heath:** Writing – review & editing, Project administration, Funding acquisition.

## Declaration of Generative AI and AI-assisted technologies in the writing process

For the preparation of this manuscript, the authors employed Quillbot and Grammarly to enhance the language and clarity of the document and restructure the sentences therein. After using these tools, the authors reviewed and edited the content as deemed necessary and take complete responsibility for the content of the published article.

## Declaration of Competing Interest

The authors declare that they have no known competing financial interests or personal relationships that could have appeared to influence

the work reported in this paper.

## Acknowledgements

Authors acknowledge the support of "FoodTraNet" MSCA-ITN project, and the funding received from the European Union's Horizon 2020 research and innovation program under the Marie Skłodowska-Curie grant agreement No. 956265 and the Project PID2023–147846OB-C21 under the Spanish Ministry of Science, Innovation and Universities. This work was also financially supported by the Slovenian Research and Innovation Agency (ARIS): Project No. L7–4422, J2–4427, L2–1830, and programmes PR-11499, P1–0143 and P2–0084. The authors would like to thank Dr. David Heath of the Department of Environmental Sciences, Jožef Stefan Institute, for his careful English language editing of the manuscript.

## Appendix A. Supporting information

Supplementary data associated with this article can be found in the online version at doi:10.1016/j.ecoenv.2026.119873.

## Data availability

Data will be made available on request.

## References

Agius, C., Von Tucher, S., Poppenberger, B., Rozhon, W., 2018. Quantification of sugars and organic acids in tomato fruits. MethodsX 5, 537–550. https://doi.org/10.1016/j.mex.2018.05.014.

Bolea-Fernandez, E., Rua-Ibarz, A., Velimirovic, M., Tirez, K., Vanhaecke, F., 2020. Detection of microplastics using inductively coupled plasma-mass spectrometry (ICP-MS) operated in single-event mode. J. Anal. At. Spectrom. 35 (3), 455–460. https://doi.org/10.1039/C9JA00379G.

Büks, F., Kaupenjohann, M., Dec. 2020. Global concentrations of microplastics in soils – a review. SOIL 6 (2), 649–662. https://doi.org/10.5194/soil-6-649-2020.

G.C. Caceres, M.E. Johnson, J.L. Molloy, S.B. Lee, and A.R. Montoro Bustos, Extending the Linear Dynamic Range of Single Particle ICP-MS for the Quantification of Microplastics, Anal. Chem., vol. 97, no. 36, pp. 19818–19828, doi: 10.1021/acs.analchem.5c03552.

Chialva, M., et al., 2019. Understanding changes in tomato cell walls in roots and fruits: the contribution of arbuscular mycorrhizal colonization. Int. J. Mol. Sci. 20 (2), 415. https://doi.org/10.3390/ijms20020415.

Crosset-Perrotin, G., et al., 2025. Production, labeling, and applications of micro- and nanoplastic reference and test materials. Environ. Sci. Nano 12 (6), 2911–2964. https://doi.org/10.1039/D4EN00767K.

Dahal, D., Pich, A., Braun, H.P., Wydra, K., 2010. Analysis of cell wall proteins regulated in stem of susceptible and resistant tomato species after inoculation with Ralstonia solanacearum: a proteomic approach. Plant Mol. Biol. 73 (6), 643–658. https://doi.org/10.1007/s11103-010-9646-z.

Dan, Y., Zhang, W., Xue, R., Ma, X., Stephan, C., Shi, H., 2015. Characterization of gold nanoparticle uptake by tomato plants using enzymatic extraction followed by single-particle inductively coupled plasma–mass spectrometry analysis. Environ. Sci. Technol. 49 (5), 3007–3014. https://doi.org/10.1021/es506179e.

Directive - EU - 2024/3019 - EN - EUR-Lex." Accessed: Mar. 25, 2025. [Online]. Available: ⟨https://eur-lex.europa.eu/eli/dir/2024/3019/oj/eng⟩.

Dong, Y., Gao, M., Qiu, W., Song, Z., 2021. Uptake of microplastics by carrots in presence of As (III): Combined toxic effects. J. Hazard. Mater. 411, 125055. https://doi.org/10.1016/j.jhazmat.2021.125055.

Enders, K., Lenz, R., Beer, S., Stedmon, C.A., 2017. Extraction of microplastic from biota: recommended acidic digestion destroys common plastic polymers. ICES J. Mar. Sci. 74 (1), 326–331. https://doi.org/10.1093/icesjms/fsw173.

FAO, 2021. Assessment of Agricultural Plastics and Their Sustainability: A Call for Action. FAO. https://doi.org/10.4060/cb7856en.

Giorgetti, L., et al., 2020a. Exploring the interaction between polystyrene nanoplastics and Allium cepa during germination: Internalization in root cells, induction of toxicity and oxidative stress. Plant Physiol. Biochem 149, 170–177. https://doi.org/10.1016/j.plaphy.2020.02.014.

Giorgetti, L., et al., 2020b. Exploring the interaction between polystyrene nanoplastics and Allium cepa during germination: Internalization in root cells, induction of toxicity and oxidative stress. Plant Physiol. Biochem 149, 170–177. https://doi.org/10.1016/j.plaphy.2020.02.014.

Gong, W., et al., 2021. Species-dependent response of food crops to polystyrene nanoplastics and microplastics. Sci. Total Environ. 796, 148750. https://doi.org/10.1016/j.scitotenv.2021.148750.

Guo, S., et al., 2023. Organic fertilizer and irrigation water are the primary sources of microplastics in the facility soil, Beijing. Sci. Total Environ. 895, 165005. https://doi.org/10.1016/j.scitotenv.2023.165005.

Jiang, X., Chen, H., Liao, Y., Ye, Z., Li, M., Klobučar, G., 2019. Ecotoxicity and genotoxicity of polystyrene microplastics on higher plant Vicia faba. Environ. Pollut. 250, 831–838. https://doi.org/10.1016/j.envpol.2019.04.055.

Jiménez-Lamana, J., Wojcieszek, J., Jakubiak, M., Asztemborska, M., Szpunar, J., 2016. Single particle ICP-MS characterization of platinum nanoparticles uptake and bioaccumulation by Lepidium sativum and Sinapis alba plants. J. Anal. At. Spectrom. 31 (11), 2321–2329. https://doi.org/10.1039/C6JA00201C.

Kedzierski, M., Cirederf-Boulant, D., Palazot, M., Yvin, M., Bruzaud, S., 2023. Continents of plastics: an estimate of the stock of microplastics in agricultural soils. Sci. Total Environ. 880, 163294. https://doi.org/10.1016/j.scitotenv.2023.163294.

Keller, A.A., Huang, Y., Nelson, J., 2018. Detection of nanoparticles in edible plant tissues exposed to nano-copper using single-particle ICP-MS. J. Nanopart. Res. 20 (4), 101. https://doi.org/10.1007/s11051-018-4192-8.

Kim, D., et al., 2022. Translocation and chronic effects of microplastics on pea plants (Pisum sativum) in copper-contaminated soil. J. Hazard. Mater. 436, 129194. https://doi.org/10.1016/j.jhazmat.2022.129194.

Kińska, K., Jiménez-Lamana, J., Kowalska, J., Krasnodębska-Ostręga, B., Szpunar, J., 2018. Study of the uptake and bioaccumulation of palladium nanoparticles by Sinapis alba using single particle ICP-MS. Sci. Total Environ. 615, 1078–1085. https://doi.org/10.1016/j.scitotenv.2017.09.203.

Kokko, L., Lövgren, T., Soukka, T., 2007. Europium(III)-chelates embedded in nanoparticles are protected from interfering compounds present in assay media. Anal. Chim. Acta 585 (1), 17–23. https://doi.org/10.1016/j.aca.2006.12.006.

Laborda, F., Jiménez-Lamana, J., Bolea, E., Castillo, J.R., 2013. Critical considerations for the determination of nanoparticle number concentrations, size and number size distributions by single particle ICP-MS. J. Anal. At. Spectrom. 28 (8), 1220–1232. https://doi.org/10.1039/C3JA50100K.

Lai, Y., Xu, A., Dong, L., Li, S., Li, Y., Liu, J., 2025. Quantitative tracking of nanoplastic uptake and distribution in zebrafish by single-particle inductively coupled plasma mass spectrometry. Anal. Chem. 97 (49), 27298–27307. https://doi.org/10.1021/acs.analchem.5c05336.

Larbat, R., Paris, C., Le Bot, J., Adamowicz, S., 2014. Phenolic characterization and variability in leaves, stems and roots of Micro-Tom and patio tomatoes, in response to nitrogen limitation. Plant Sci. Int. J. Exp. Plant Biol. 224, 62–73. https://doi.org/10.1016/j.plantsci.2014.04.010.

Lee, S., Bi, X., Reed, R.B., Ranville, J.F., Herckes, P., Westerhoff, P., 2014. Nanoparticle size detection limits by single particle ICP-MS for 40 elements. Environ. Sci. Technol. 48 (17), 10291–10300. https://doi.org/10.1021/es502422v.

Li, C., et al., 2021b. Quantification of nanoplastic uptake in cucumber plants by pyrolysis gas chromatography/mass spectrometry. Environ. Sci. Technol. Lett. 8 (8), 633–638. https://doi.org/10.1021/acs.estlett.1c00369.

Li, L., et al., 2020. Effective uptake of submicrometre plastics by crop plants via a crack-entry mode. Nat. Sustain 3 (11), 929–937. https://doi.org/10.1038/s41893-020-0567-9.

Li, Y., Lin, X., Wang, J., Xu, G., Yu, Y., 2023. Quantification of nanoplastics uptake and transport in lettuce by pyrolysis gas chromatography-mass spectrometry. Talanta 265, 124837. https://doi.org/10.1016/j.talanta.2023.124837.

Li, Z., Li, Q., Li, R., Zhou, J., Wang, G., 2021a. The distribution and impact of polystyrene nanoplastics on cucumber plants. Environ. Sci. Pollut. Res. 28 (13), 16042–16053. https://doi.org/10.1007/s11356-020-11702-2.

Lian, J., et al., 2021. Foliar-applied polystyrene nanoplastics (PSNPs) reduce the growth and nutritional quality of lettuce (Lactuca sativa L.). Environ. Pollut. 280, 116978. https://doi.org/10.1016/j.envpol.2021.116978.

Liang, R.-L., et al., 2015. Rapid and sensitive lateral flow immunoassay method for determining alpha fetoprotein in serum using europium (III) chelate microparticles-based lateral flow test strips. Anal. Chim. Acta 891, 277–283. https://doi.org/10.1016/j.aca.2015.07.053.

Liu, Y., Guo, R., Zhang, S., Sun, Y., Wang, F., 2022. Uptake and translocation of nano/microplastics by rice seedlings: Evidence from a hydroponic experiment. J. Hazard. Mater. 421, 126700. https://doi.org/10.1016/j.jhazmat.2021.126700.

Luo, Y., et al., 2022a. Quantitative tracing of uptake and transport of submicrometre plastics in crop plants using lanthanide chelates as a dual-functional tracer. Nat. Nanotechnol. 17 (4). https://doi.org/10.1038/s41565-021-01063-3.

Luo, Y., et al., 2022b. Quantitative tracing of uptake and transport of submicrometre plastics in crop plants using lanthanide chelates as a dual-functional tracer. Nat. Nanotechnol. 17 (4), 424–431. https://doi.org/10.1038/s41565-021-01063-3.

Maddela, N.R., Ramakrishnan, B., Kadiyala, T., Venkateswarlu, K., Megharaj, M., 2023. Do microplastics and nanoplastics pose risks to biota in agricultural ecosystems? Soil Syst. 7 (1). https://doi.org/10.3390/soilsystems7010019.

Mahakun, N., Leeper, P.W., Burns, E.E., 1979. Acidic constituents of various tomato fruit types. J. Food Sci. 44 (4), 1241–1244. https://doi.org/10.1111/j.1365-2621.1979.tb03489.x.

Mitrano, D.M., Beltzung, A., Frehland, S., Schmiedgruber, M., Cingolani, A., Schmidt, F., 2019. Synthesis of metal-doped nanoplastics and their utility to investigate fate and behavior in complex environmental systems. Nat. Nanotechnol. 14 (4), 362–368. https://doi.org/10.1038/s41565-018-0360-3.

OECD, Global Plastics Outlook: Policy Scenarios to 2060, oecd-ilibrary.org. Accessed: Jun. 10, 2024. [Online]. Available: https://read.oecd-ilibrary.org/environment/global-plastics-outlook_aa1edf33-en.

J.W. Park, S.J. Lee, D.Y. Hwang, and S. Seo, Removal of microplastics via tannic acid-mediated coagulation and in vitro impact assessment, RSC Adv., vol. 11, no. 6, pp. 3556–3566, doi: 10.1039/d0ra09645h.

Pérez-Reverón, R., González-Sálamo, J., Hernández-Sánchez, C., González-Pleiter, M., Hernández-Borges, J., Díaz-Peña, F.J., 2022. Recycled wastewater as a potential source of microplastics in irrigated soils from an arid-insular territory

(Fuerteventura, Spain). Sci. Total Environ. 817, 152830. https://doi.org/10.1016/j.scitotenv.2021.152830.
Ragoobur, D., Huerta-Lwanga, E., Somaroo, G.D., 2021. Microplastics in agricultural soils, wastewater effluents and sewage sludge in Mauritius. Sci. Total Environ. 798, 149326. https://doi.org/10.1016/j.scitotenv.2021.149326.
H.M. Resh, Hydroponic Food Production: A Definitive Guidebook for the Advanced Home Gardener and the Commercial Hydroponic Grower. Accessed: Feb. 10, 2025. [Online]. Available: ⟨https://www.routledge.com/Hydroponic-Food-Production-A-Definitive-Guidebook-for-the-Advanced-Home-Gardener-and-the-Commercial-Hydroponic-Grower/Resh/p/book/9780367678753⟩.
Sahai, H., et al., 2025. Key insights into microplastic pollution in agricultural soils: A comprehensive review of worldwide trends, sources, distribution, characteristics and analytical approaches. TrAC Trends Anal. Chem. 185, 118176. https://doi.org/10.1016/j.trac.2025.118176.
Sahai, H., Bueno, M.J.M., Del Mar Gómez-Ramos, M., Fernández-Alba, A.R., Hernando, M.D., 2024. Quantification of nanoplastic uptake and distribution in the root, stem and leaves of the edible herb Lepidum sativum. Sci. Total Environ. 912, 168903. https://doi.org/10.1016/j.scitotenv.2023.168903.
Seufert, P., Staiger, S., Arand, K., Bueno, A., Burghardt, M., Riederer, M., 2022. Building a barrier: the influence of different wax fractions on the water transpiration barrier of leaf cuticles. Front. Plant Sci. 12. https://doi.org/10.3389/fpls.2021.766602.
Silva-Beltrán, N.P., et al., 2015. Total phenolic, flavonoid, tomatine, and tomatidine contents and antioxidant and antimicrobial activities of extracts of tomato plant. Int. J. Anal. Chem. 2015 (1), 284071. https://doi.org/10.1155/2015/284071.
Sun, H., Lei, C., Xu, J., Li, R., 2021. Foliar uptake and leaf-to-root translocation of nanoplastics with different coating charge in maize plants. J. Hazard. Mater. 416, 125854. https://doi.org/10.1016/j.jhazmat.2021.125854.
Sun, X.-D., et al., 2020. Differentially charged nanoplastics demonstrate distinct accumulation in Arabidopsis thaliana. Nat. Nanotechnol. 15 (9). https://doi.org/10.1038/s41565-020-0707-4.
Taylor, S.E., et al., 2020. Polystyrene nano- and microplastic accumulation at Arabidopsis and wheat root cap cells, but no evidence for uptake into roots. Environ. Sci. Nano 7 (7), 1942–1953. https://doi.org/10.1039/D0EN00309C.
Tian, L., Jinjin, C., Ji, R., Ma, Y., Yu, X., 2022. Microplastics in agricultural soils: sources, effects, and their fate. Curr. Opin. Environ. Sci. Health 25, 100311. https://doi.org/10.1016/j.coesh.2021.100311.
Tympa, L.-E., Katsara, K., Moschou, P.N., Kenanakis, G., Papadakis, V.M., 2021. Do microplastics enter our food chain via root vegetables? A Raman based spectroscopic study on *Raphanus sativus*. Materials 14 (9). https://doi.org/10.3390/ma14092329.
Wang, J., et al., 2022. Uptake and bioaccumulation of nanoparticles by five higher plants using single-particle-inductively coupled plasma-mass spectrometry. Environ. Sci. Nano 9 (8), 3066–3080. https://doi.org/10.1039/D1EN01195B.
Wang, Y., et al., 2024. Tracking and imaging nano-plastics in fresh plant using cryogenic laser ablation inductively coupled plasma mass spectrometry. J. Hazard. Mater. 465, 133029. https://doi.org/10.1016/j.jhazmat.2023.133029.
Wei, W.-J., et al., 2021. Enzyme digestion combined with SP-ICP-MS analysis to characterize the bioaccumulation of gold nanoparticles by mustard and lettuce plants. Sci. Total Environ. 777, 146038. https://doi.org/10.1016/j.scitotenv.2021.146038.
Weissman, S.I., 1942. Intramolecular energy transfer the fluorescence of complexes of europium. J. Chem. Phys. 10 (4), 214–217. https://doi.org/10.1063/1.1723709.
Yu, Z., Xu, X., Guo, L., Jin, R., Lu, Y., 2024. Uptake and transport of micro/nanoplastics in terrestrial plants: Detection, mechanisms, and influencing factors. Sci. Total Environ. 907, 168155. https://doi.org/10.1016/j.scitotenv.2023.168155.
Zhang, T.-R., et al., 2019. Uptake and translocation of styrene maleic anhydride nanoparticles in *Murraya exotica* plants as revealed by noninvasive, real-time optical bioimaging. Environ. Sci. Technol. 53 (3), 1471–1481. https://doi.org/10.1021/acs.est.8b05689.
Zhou, J., Xia, R., 2024. Leafy vegetable assimilation of atmospheric microplastics/nanoplastics: an overlooked source in human food? Environ. Sci. Technol. Lett. 11 (2), 51–53. https://doi.org/10.1021/acs.estlett.3c00887.